54. Computational Neurogenetic Modeling: Gene-Dependent Dynamics of Cortex and Idiopathic Epilepsy

Lubica Benuskova, Nikola Kasabov

The chapter describes a novel computational approach to modeling the cortex dynamics that integrates gene–protein regulatory networks with a neural network model. Interaction of genes and proteins in neurons affects the dynamics of the whole neural network. We have adopted an exploratory approach of investigating many randomly generated gene regulatory matrices out of which we kept those that generated interesting dynamics. This naïve brute force approach served us to explore the potential application of computational neurogenetic models in relation to gene knock-out experiments. The knock out of a hypothetical gene for fast inhibition in our artificial genome has led to an interesting neural activity. In spite of the fact that the artificial gene/protein network has been altered due to one gene knock out, the dynamics of SNN in terms of spiking activity was most of the time very similar to the result obtained with the complete gene/protein network. However, from time to time the neurons spontaneously temporarily synchronized their spiking into coherent global oscillations. In our model, the fluctuations in the values of neuronal parameters leads to spontaneous development of seizure-like global synchronizations. These very same fluctuations also lead to termination of the seizure-like neural activity and maintenance of the inter-ictal normal periods of activity. Based on our model, we would like to suggest a hypothesis that parameter changes due to the gene–protein dynamics should also be included as a serious factor determining transitions in neural dynamics, especially when the cause of disease is known to be genetic.

54.1 Overview

Properties of all cell types, including neurons, are determined by proteins they contain [54.1]. In turn, the types and levels of proteins are determined by differential transcription of genes in response to internal and

external signals. Eventually, the properties of neurons determine the structure and dynamics of the whole neural network they are part of. In this chapter, we turn our attention to modeling the influence of genes and proteins upon the dynamics of mature cortex and the dynamic effects due to mutations of genes. The chapter is thus an extension and further development of a general framework for modeling brain functions and genetically caused dysfunctions by means of computational neurogenetic modeling [54.2].

54.1.1 Neurogenesis

Sophisticated mathematical and computer models of the general control of gene expression during early embryonic development of neural system in vertebrates have been developed [54.3]. Computational models based on the analogy of gene regulatory networks with artificial neural networks have been applied to model the steps in *Drosophila* early neurogenesis [54.4, 5]. The latter models attempted to elucidate how genes orchestrate the detailed pattern of early neural development. During early development, dynamics of changes in architecture and morphology of neural network parallels changes in gene expression in time.

54.1.2 Circadian Rhythms

One particular instance where the gene expression determines the neural dynamics is the circadian rhythm. A circadian rhythm is a roughly-24 h cycle in the physiological processes of plants and animals. The circadian rhythm partly depends on external cues such as sunlight and temperature, but otherwise it is determined by periodic expression patterns of the so-called clock genes [54.6, 7]. *Smolen* et al. [54.8] have developed a computational model to represent the regulation of core clock component genes in *Drosophila* (*per*, *vri*, *Pdp-1*, and *Clk*). To model the dynamics of gene expression, differential equations and first-order kinetics equations were employed for modeling the control of genes and their products. The model illustrates the ways in which negative and positive feedback loops within the gene regulatory network (GRN) cooperate to generate oscillations of gene expression. The relative amplitudes and phases of simulated oscillations of gene expressions resemble empirical data in most simulated situations. The model of *Smolen* et al. [54.8] shows that it is possible to develop detailed models of gene control of neural behavior provided that enough experimental data is available to adjust the model.

54.1.3 Neurodegenerative Diseases

Many diseases that affect the central nervous system and manifest cognitive symptoms have an underlying genetic cause – some are due to a mutation in a single gene, others are proving to have a more complex mode of inheritance [54.9]. A large group of disorders are neurodegenerative disorders (like Alzheimer's disease, Rett syndrome, Huntington disease, etc.), in which the underlying gene mutations lead to particular degenerative processes in the brain that progressively affect neural functions and eventually have fatal consequences. In the case of neurodegenerative diseases, the dynamics of neural networks degeneration is slow, usually lasting for years. The gene mutation is always there and particular degenerative changes in the brain tissue accumulate over time. It is a challenge for future computational neurogenetic-genetic models to attempt to model the onset and progression of these diseases using the integration of gene regulatory networks and artificial neural networks. Already for Alzheimer's disease, computational models of neural networks' dysfunction caused by experimentally identified biochemical factors that result from genetic abnormalities have been developed to gain insights into the neural symptoms of the disease [54.10–12]. All these neurodegenerative diseases (like Alzheimer's disease, Rett syndrome, Huntington disease, etc.) are characterized by the fact that once the gene mutation manifests itself, the disease progresses and its symptoms of cognitive impairment are always there.

54.1.4 Idiopathic Epilepsies

However, there are genetic diseases of the brain like, for instance, some genetically caused epilepsies, in which the main symptom – seizure – occurs only from time to time and between these episodes, in fact most of the time, the brain activity appears normal. In general, epilepsy is a disorder characterized by the occurrence of at least two unprovoked seizures [54.13]. Seizures are the manifestation of abnormal hypersynchronous discharges of neurons in the cerebral cortex. The clinical signs or symptoms of seizures depend on the location and extent of the propagation of the discharging cortical neurons. The prevalence of active epilepsy is about 1% [54.13], which, however, means about 70 million people worldwide are affected. Seizures are often a common manifestation of neurologic injury and disease, which should not be surprising because the main function of neurons is the transmission of elec-

trical impulses. Thus, most epilepsies are not caused genetically. A particular case of nongenetic epilepsy is temporal lobe epilepsy (TLE). The most common pathological finding in TLE is hippocampal (temporal lobe) sclerosis that involves cell loss [54.14]. High-resolution MRI shows hippocampal atrophy in 87% of patients with TLE. Causes of the cell loss involve: past infections, trauma, and vascular and brain tissue malformations including tumors. Experimentally, the specific cell loss can be triggered by the injection of kainic acid [54.15]. Inhibitory neurons are more affected than excitatory neurons. Two broad classes of GABAergic inhibitory neurons can be distinguished: (1) dendritic-projecting interneurons mediating the slow inhibition through the $GABA_B$ and $GABA_A$ dendritic postsynaptic receptors [54.16, 17], and (2) interneurons that selectively innervate somas of other neurons and mediate the fast inhibition through $GABA_A$ type of postsynaptic receptors [54.15, 18]). In TLE, a selective reduction of the slow (dendritic) inhibition and an increase in the fast (somatic) inhibition have been identified [54.15]. There are many computational models of temporal lobe-like epileptic seizures based on the effect of abnormal values of inhibition parameters upon neural network dynamics [54.19–22].

There is quite a high percentage of pharmacoresistant epilepsies, i. e., 15–50% depending on age and definition [54.23]. In humans with intractable temporal lobe epilepsy (TLE), many of surviving inhibitory interneurons lose their PV content or PV immunoreactivity [54.24]. It has been proposed that efficient Ca^{2+} buffering by PV and its high concentration in PV-expressing inhibitory cells is a prerequisite for the proficient inhibition of cortical networks [54.25]. To investigate this hypothesis, Schwaller and co-workers used mice lacking PV ($PV^{-/-}$). These mice show no obvious abnormalities and do not have epilepsy [54.26]. However, the severity of generalized tonic-clonic seizures induced by pentylenetetrazol (PTZ) was significantly greater in $PV^{-/-}$ than in $PV^{+/+}$ animals. Extracellular single-unit activity recorded from over 1000 neurons *in vivo* in the temporal cortex revealed an increase of units firing regularly and a decrease of cells firing in bursts. In addition, control animals showed a lesser degree of synchronicity and mainly high frequency components above 65 Hz in the local field potential (LFP) spectrum compared to $PV^{-/-}$ mice. On the other hand, $PV^{-/-}$ mice were characterized by increased synchronicity and by abnormally high proportion of frequencies below 40 Hz [54.27]. In the hippocampus, PV deficiency facilitated the $GABA_A$ergic current reversal induced by high-frequency stimulation, a mechanism implied in the generation of epileptic activity [54.28]. Through an increase in inhibition, the absence of PV facilitates hypersynchrony through the depolarizing action of GABA [54.26]. Thus there is a permanent change in the spectrum of the local field potential (LFP) of the PV gene KO mice. We developed a hierarchical spiking neural network model of LFP, in which each neuron has the values of parameters governed by an internal gene regulatory network [54.29]. For simplicity and because the measurements of LFP lasted only minutes, we assumed the gene expressions were constant. In spite of that, the removal of the gene for PV from the gene regulatory network affected all the parameters of neurons. We have evolved the gene interactions so that the resulting gene interaction matrix yielded such values of neuronal parameters that the resulting model LFP had similar changes of the frequency spectrum as in the experiment with $PV^{-/-}$ mice of *Villa* et al. [54.27].

Genetic contribution to etiology has been estimated to be present in about 40% of patients with epilepsy [54.30]. Pure Mendelian epilepsies, in which a single major locus can account for segregation of the disease trait are considered to be rare and probably account for no more than 1% of patients [54.30]. The common familial epilepsies tend to display complex inheritance, in which the pattern of familial clustering can be accounted for by the interaction of several loci together with environmental factors. Table 54.1 lists some types of genetically caused epilepsies, associated brain pathologies, symptoms, and putative mutated genes. This account is by far not complete.

54.1.5 Computational Models of Epilepsies

Let us consider in more detail childhood absence epilepsy (CAE). It is an idiopathic (i. e., arising from an unknown cause), generalized nonconvulsive epilepsy [54.31, 32]. The main feature is absence seizures. A typical absence is a nonconvulsive epileptic seizure, characterized by a briefly (4–20 s) lasting impairment of consciousness. This may happen up to about eight times each hour, and up to ≈ 200 times a day. Absence seizures occur spontaneously, i. e., they are not evoked by sensory or other stimuli. Absence is accompanied by a generalized, synchronous, bilateral, 2.5–4 Hz spike and slow-wave discharge (SWD) with large amplitudes in the electroencephalogram (EEG), see Fig. 54.1.

SWDs can start anywhere in the cortex and from there they quickly spread to the entire cortex and thalamus [54.33]. The origin can also be in the thala-

Table 54.1 Some idiopathic epilepsies, putative mutated genes, and affected functions of brain neurons in humans

Epilepsy	Mutated genes/chromosome location (if known)	Brain abnormality	Symptoms	References
Autosomal dominant nocturnal frontal lobe epilepsy (ADNFL)	α_4 subunit of the nicotinic AchR (CHRNA4)/20q β_2 subunit of the same receptor (CHRNB2)/1p	Reduced nAchR channel opening time and reduced conductance leading to hyperexcitability	Partial seizures during night that may generalize, arising from the frontal lobes, motor, tonic, postural type	[54.36–38]
Benign familial neonatal convulsions (BFNC1 and BFNC2)	EBN1 (K^+ channel gene KCQ2)/20q EBN2 (K^+ channel gene KCNQ3)/8q	Alteration of the gating properties of the K^+ channel leading to poor control of repetitive firing	Generalized epilepsy of newborns, seizures are frequent and brief, episodes resolve within a few days	[54.36–39]
Childhood absence epilepsy (CAE)	γ_2 subunit gene for the $GABA_A$ receptor gene GABRG2/5q gene CLCN2/3q	Fast and part of slow GABAergic inhibition is reduced, voltage-gated Cl^- channel function is impaired	Absence seizures (consciousness impaired) up to 200 times a day, bilateral 2–4 Hz spike and slow-wave EEG	[54.31, 32]
Generalized epilepsy and febrile seizures plus (GEFS+)	β_1 subunit of the Na^+ channel gene SCN1B/19q α_1 and α_2 subunits, gene SCN1A and gene SCN2A/2q GABRG2/5q	Normal inactivation kinetics of the Na^+ channel is reduced causing persistent Na^+ influx and hyperexcitability, reduced function of the $GABA_AR$	Childhood onset of febrile seizures, with febrile and afebrile generalized seizures continuing beyond 6 years of age	[54.36–38]
Intractable childhood epilepsy	α_1 subunit of the Na^+ channel, gene SCN1A/2q	Rapid recovery of the Na^+ channel from inactivation or very slow inactivation	Frequent intractable generalized tonic-clonic seizures	[54.39]
Juvenile absence epilepsy (JAE)	α_1/5q, α_5/15q, γ_2/5q subunit genes for the $GABA_A$ receptor gene (CLCN2)/3q	Fast and part of slow GABAergic inhibition is reduced, voltage-gated Cl channel function is impaired	Similar like CAE but the seizures start after year 10, seizures may be less frequent and last longer than few seconds	[54.39]
Juvenile myoclonic epilepsy (JME)	α_7 subunit of the nicotinic AchR (CHRNA7)/15q gene CLCN2/3q, β_4 subunit of Ca^{2+} channel, (CACNB4)/19p	Reduced function of the nicotinic AChR, voltage-gated Cl channel and voltage-gated Ca^{2+} channel have reduced conductance	Myoclonic jerks or seizures shortly after awakening, generalized tonic-clonic seizures, and sometimes absence seizures	[54.36]
Dravet syndrome, severe myoclonic epilepsy of infancy (SMEI)	α_1 subunit of the Na^+ channel, gene SCN1A/2q	Complete loss of activity of the Na^+ channel	Both generalized and localized seizures, clonic and myoclonic seizure types	[54.38, 39]
Lafora disease (progressive myoclonus epilepsy)	Laforin gene EPM2A/6q24 malin gene EPM2B/6p22.3	Presence of Lafora bodies (granules of accumulated carbohydrates)	Myoclonic jerking, ataxia, mental deterioration leading to dementia	[54.40]

mus [54.34]. Several gene mutations have been reported for CAE, and an extensive review can be found, for instance, in [54.31]. Some suspected gene mutations are linked to the receptor $GABA_A$ which mediates the so-called fast somatic inhibition and a smaller part of the slow dendritic inhibition in the cortex [54.16, 17]. Blockage of $GABA_A$ receptors by chemical agents leads to SWDs even in healthy brain tissue and in the corresponding model of the thalamo-cortical circuit [54.18, 34]. If excitatory and inhibitory cells generate high-frequency discharges in synchrony and if $GABA_B$ receptors are present (their time constants match with the period of SWDs), sufficient conditions are brought together to generate SWDs. In computational models, epileptic discharges can be evoked *chemically* or by a specifically manipulated input, and these seizures last as long as this altered input or chemical is present [54.20, 35]. However, in reality seizures occur *spontaneously* during the alert state of the brain (that is in CAE). The underlying cause is always there,

i. e., the gene mutation, however, the seizures are not always present. When a spiking neural network model is used to model epilepsy, it can be shown that spiking neurons in a network exhibit spontaneous synchronizations when the overall excitation is permanently increased [54.22]. Depending on the level of total excitation of neurons the model network went from the nonbursting (asynchronous) activity through single synchronized bursts each lasting few milliseconds, and complex partly synchronized clusters of bursts, each lasting few seconds, to a continuous synchronization of firing. However in this model, the *ictal* and *inter-ictal* periods are unrealistically short, i. e., both periods lasting few seconds at most. While in CAE the seizures are indeed short-lasting, the inter-seizure periods are generally longer than just few seconds.

Although the above models cast invaluable insights into the mechanisms underlying epilepsies, according to us, these models do not satisfactorily explain spontaneous transitions to and from the seizures, neither the maintenance of inter-ictal and ictal states. Noise can be used to trigger transitions to and from abnormal activity, but cannot dramatically change the short duration of periodic and aperiodic phases of activity (being on the order of milliseconds – our own simulations of spiking networks). The reason is that these models work with constant values of parameters. We believe that if the parameter values were allowed to change dynamically, more realistic temporal dynamics could be achieved. *LeMasson, Marder* and *Abbott* [54.41,42], realized that in neurons, like in other cells, there is a continuous turnover of ion channels and receptors that underlie neuronal signaling such that the properties of neurons are dynamically modified. They investigated the role of neuronal activity upon dynamic modification and maintenance of neuronal conductances to achieve a biologically plausible explanation of transitions between different neural activity modes in the stomatogastric ganglion. In their models the activity-dependent intracellular calcium concentration was used as a feedback element that leads to processes of insertion, removal, and modification of ion channels. These processes, happening probably at a local synaptic level, can be quite fast, taking just seconds or at most minutes, because they do not involve gene expression.

54.1.6 Outline of the Chapter

So far, due to the complexity of the whole issue, no attempt to bridge the slow dynamics of gene–protein-gene interactions with the fast dynamics of neural networks has been made. We think it can be done and we would like to elaborate a proposal of how to move forward in this direction. Thus, in this chapter we describe a computational neurogenetic model (CNGM) to investigate the influence of a slow gene–protein dynamics upon the fast neural dynamics. This approach is illustrated by means of a simple model of a spiking neural network, in which parameter values are linked to proteins that are the products of gene expression. Gene expressions change in time as a consequence of the dynamics of the internal gene–protein regulatory network. Thus, the values of neuronal parameters are not fixed but instead they vary in time due to the changes in expressions of genes coding for proteins that are behind the corresponding parameters of the neuronal functions (like amplitude of excitation or inhibition, resting firing threshold, etc.). In such a way, we can investigate different modes of gene interactions with normal or knock out genes, and their effects upon the neural dynamics. Based on these toy simulations we propose a hypothesis that spontaneous transitions to and from the ictal neural activity may be due to variations of neuronal parameters resulting from the underlying dynamics of gene–protein regulatory interactions. In other words, we would like to suggest a hypothesis why the seizures occur only from time to time and why between these episodes, in fact most of

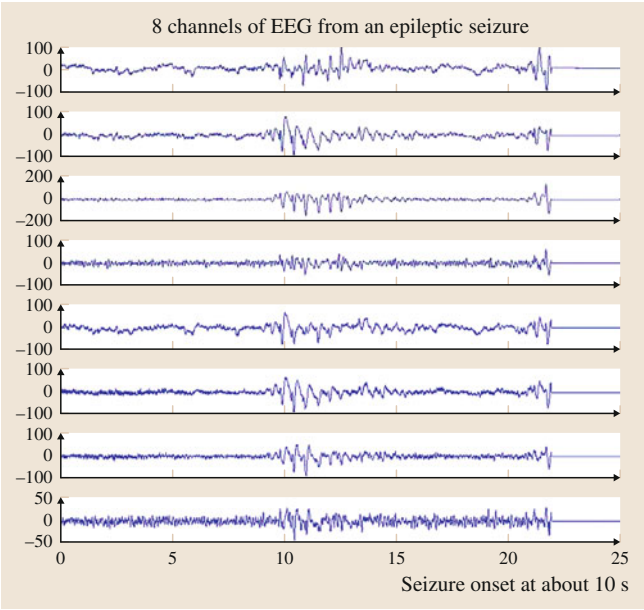

Fig. 54.1 EEG record of eight channels of the normal and epileptic slow-wave discharge (SWD) in childhood absence epilepsy. SWD have large amplitudes and frequency of 2.5–4 Hz

the time, the brain activity appears normal in spite of the genetic mutation always being present.

First we overview relevant facts from molecular biology and bioinformatics. Then we introduce the model that is a continuous extension of the discrete model of gene–protein dynamics introduced in [54.43, 44]. Next we present some illustrative computer simulations with the new continuous model. In the discussion section, we outline directions for further development and applications of the neurogenetic approach to future modeling of the genetic brain disorders.

54.2 Gene Expression Regulation

54.2.1 Protein Synthesis

The term gene expression refers to the entire process whereby the information encoded in a particular (protein-coding) gene is decoded into a particular protein [54.1]. Regulation at any one of the various steps in this process can lead to differential gene expression in different cell types, different developmental stages of one cell type, in response to external conditions, etc. The most important mechanism for determining whether or not most genes are expressed is the control of transcription initiation [54.1].

After transcription has been initiated, RNA polymerase II, together with the necessary transcription elongation factors, travels along the DNA template and polymerizes ribonucleotides into a pre-messenger RNA (pre-mRNA) copy of the gene. The polymerase moves at a regular speed (approximately 30–50 nucleotides per second) and holds on to the DNA template efficiently, even if the gene is very long. At the end of the gene, the RNA polymerase falls off the DNA template and transcription terminates [54.45]. Each resulting pre-mRNA consists of two types of segments – exons, that are segments translated into proteins, and introns – segments that are considered redundant and do not take part in the protein production. Removing the introns and ordering only the exon parts of the genes in the RNA sequence is called splicing and this process results in the production of a messenger RNA (mRNA) sequence. From one gene, many copies of mRNA are produced that are directly translated into proteins. Each protein consists of a sequence of amino acids, each of them coded by a base triplet of the transport RNA (tRNA), called a codon. Translation of mRNA sequence into the protein sequence (by means of tRNA) occurs on ribosomes, which are the protein synthesizing machines of cells. Elongation of a protein polypeptide proceeds at a rate of 3–5 amino acids added per second [54.45].

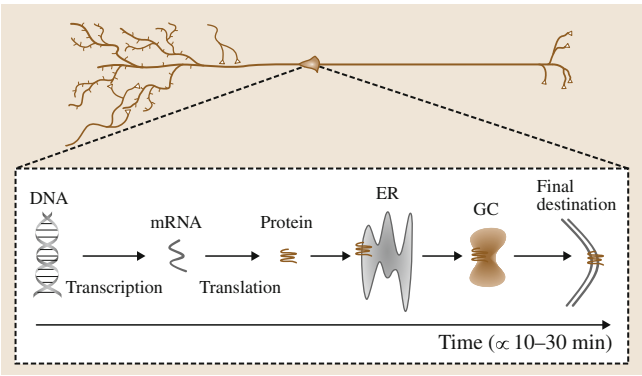

Fig. 54.2 Overview of the protein synthesis. ER = endoplasmic reticulum, GC = Golgi complex. Final destination for a protein from a secretory pathway can be, for instance, the plasmatic membrane, if it is a receptor

On average, a vertebrate gene is around 30 kb = 30 000 bases long, out of which the coding region is only about 1–2 kb = 1000–2000 bases long, that is 3–7%. However, huge deviations from the average can be observed. Thus from the initiation of transcription, it would take around 600–1000 s = 10–17 min to transcribe this average 30 kb gene. Translation of the coding part would take approximately 3–10 min. In total, the process of an average protein synthesis would last about 13–27 min. However, the process of protein preparation for its function is not over yet for the so-called proteins of the secretory pathways, like hormones, neurotransmitters, receptors, etc. [54.46]. After being synthesized on ribosomes, these proteins are transferred to endoplasmic reticulum (ER) to undergo the posttranslational modifications. After modification is completed in the ER, these proteins move via transport vesicles to the Golgi complex from where they are further sorted to several destinations, like axonal terminals, synapses, etc. The whole process is summarized in Fig. 54.2. Posttranslational modifications, sorting, and transport also take some time, probably on the order of minutes. Thus, from the initiation of transcription, it is fair to say, that it takes about 15 min

for an average protein of the secretory pathway to start functioning in its place, and it may take even more, depending on the size of the protein. It is also obvious that this time delay is different for different proteins. These temporal considerations will be important for the construction of the general gene–protein regulatory network.

54.2.2 Control of Gene Expression

Each gene has a promoter region. The binding of a nonspecific basal factor to promoter is a prerequisite for the basal level of the transcription of a gene. The differential level of transcription is controlled by transcription factors, activators and repressors, which bind to regulatory DNA sequences, located proximally to the promoter. Activators enhance gene expression while repressors suppress gene expression. Transcription can also be stimulated by control elements called enhancers that are more distant from the promoter region than the promoter-proximal elements. Enhancers include binding sites for several transcription factors. Thus, transcription from a single promoter may be regulated by binding of multiple transcription factors to alternative control elements, promoter-proximal elements and enhancers, permitting complex control of gene expression [54.1]. Moreover, there are molecules, which act as co-activators and co-repressors, that interact with activators and repressors to modify their activity. Whether or not a specific gene is expressed at a particular time is largely a consequence of the net effect of the activity of the number of transcription factors at that particular time.

To get from a particular protein in a cell to the control of expression of some gene takes many steps and thus some time. For instance, it is known that activation of the NMDA (*N*-methyl-D-aspartate) receptors in neurons causes de novo synthesis of BDNF (brain-derived neurotrophic factor) [54.47]. BDNF de novo synthesis was estimated by measuring the steady-state content of BDNF mRNA and protein at various times after NMDA treatment. NMDA elicited a time dependent increase in BDNF mRNA content, beginning at 3 h (2-fold) and lasting at least up to 8 h in vitro. However, a small, about 1.2-fold, increase was observed already after 1 h [54.47]. This means that it takes about an hour for the signal from the NMDA receptor to reach the genome, to initiate and carry out the transcription, and to synthesize enough proteins to be detected above the basal concentration. The NMDAR multiprotein complex contains 77 proteins out of which 19 participate in NMDAR signaling [54.48]. These signaling proteins mediate the effect by differential activation of different downstream effector pathways leading to the genome, for instance different mitogen-activated protein kinase (MAPK) pathways, depending on a particular signal [54.49]. Thus, in principle each protein in a cell has a way to influence transcription of genes through cascades of reactions leading to different transcriptional factors. This is the molecular basis for construction of different gene regulatory networks (GRNs) from gene expression data [54.50, 51].

54.3 Computational Neurogenetic Model

Here, we would like to mathematically formulate an extension of our computational neurogenetic model introduced in [54.43, 44], which was based on a discrete dynamics of gene regulatory network. Current extension takes into account different time scales and different time delays in the continuous dynamic system.

54.3.1 Gene–Protein Regulatory Network

Let us formulate a set of general equations for the gene–protein dynamic system (Fig. 54.3). As a first gross simplification, we will assume that every neuron has the same gene–protein regulatory network (GPRN) – that is, interactions between genes are the same in every neuron.

The following set of nonlinear delay differential equations (DDEs) was inspired by the mathematical model of *Chen and Aihara*, who also proved the general conditions of its stability and bifurcation for some simplifying assumptions [54.52]. Particular terms on the right-hand side of equations were inspired also by the *rough* network models from [54.53]. An equation similar to (54.2) for the protein (gene product) dynamics was used by [54.5] to model early neurogenesis in *Drosophila*. The linear difference form of (54.1) without decay was used by [54.54] to model mRNA levels during the rat CNS development and injury. In the following, we will consider the dynamics of genes and proteins to be continuous that is, we can describe their changes in a continuous time. We will speak about gene

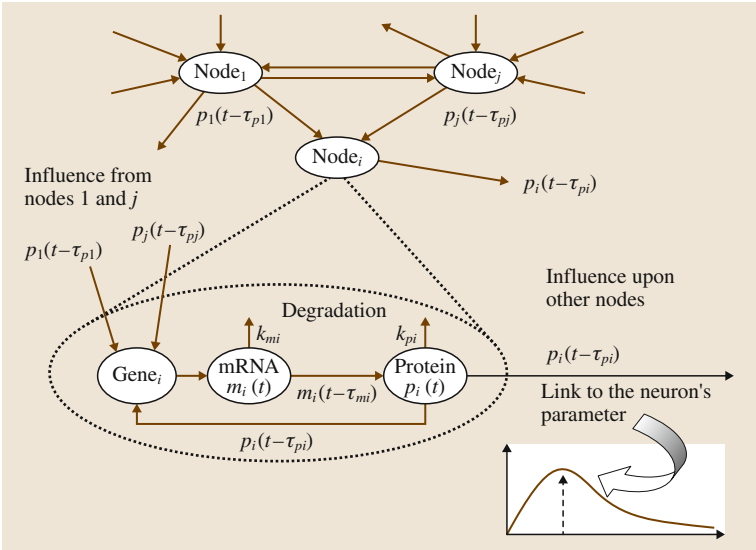

Fig. 54.3 Schematic illustration of the gene–protein regulatory network (GPRN). The edges represent regulatory interactions that lead either to up-regulation or down-regulation of expression of the target gene. These regulatory interactions are expressed as coefficients of the interaction matrix $\boldsymbol{W}$. Protein properties and concentrations are linked to neuronal parameters, like, for instance, magnitude of excitation or inhibition. GPRN illustration was inspired by the network illustration in [54.52]

families rather than individual genes. By gene families we understand the set of genes that have a coordinated transcription control and code for different subunits of one protein. These subunits have to be synthesized in concert in order to produce a functional protein. We will represent the mRNA levels of all the relevant gene families with the vector $\boldsymbol{m} = (m_1, m_2, \ldots, m_N)$ and the corresponding protein levels with the vector $\boldsymbol{p} = (p_1, p_2, \ldots, p_N)$. The level of mRNA of the gene family i changes as

$$\frac{\mathrm{d}m_i}{\mathrm{d}t} = A_{m_i}\sigma_{m_i}\left[\sum_{j=1}^{n} w_{ij}\, p_j(t-\tau_{p_j}) + \sum_{k=1}^{K} v_{ik}x_k(t-\tau_{x_k}) + b_{m_i}\right] - \lambda_{m_i} m_i(t)\,, \tag{54.1}$$

where $m_i(t)$ is the total level of mRNA for the i-th gene family at time t, σ_{m_i} is a nonlinear sigmoid regulation-expression (activation) function for the i-th gene family, A_{m_i} is the amplitude of this activation function, w_{ij} are the regulatory coefficients between the i-th and j-th gene families, while the regulatory interaction is mediated through proteins p_j, p_j is the level of the jth protein, τ_{p_j} is the delay, with which the j-th protein influences the transcription of the i-th gene family, v_{ik} is the influence of the k-th external factor upon the gene (hormone, drug, etc.), x_k is the concentration of the k-th external factor, τ_{x_k} is the delay with which the k-th external factor influences the transcription of the i-th gene family, b_{m_i} is the bias, i. e., the basal expression level of the i-th gene family, and λ_{m_i} is the degradation rate of the mRNA of the i-th gene family.

Analogically, protein levels change as

$$\frac{\mathrm{d}p_i}{\mathrm{d}t} = A_{p_i}\,\sigma_{p_i}\left[m_i(t-\tau_{m_i}) + \sum_{k=1}^{K'} u_{ik}\, y_k(t-\tau_{y_k}) + b_{p_i}\right] - \lambda_{p_i}\, p_i(t)\,, \tag{54.2}$$

where $p_i(t)$ is the level of a fully functional protein coded for by the i-th gene family, σ_{p_i} is a nonlinear sigmoid synthesis function for the i-th protein (note, we consider that one protein is coded for by only one gene family), A_{p_i} is the amplitude of this synthesis function, m_i is the total expression level of the i-th gene family, τ_{m_i} is the delay from initiation of transcription of the i-th gene family till the end of synthesis of the i-th protein (on the order of tens of minutes), u_{ik} is the influence of the k-th external factor upon the protein (hormone, drug, etc.), y_k is the concentration of the k-th external factor, τ_{y_k} is the delay with which the k-th external factor influences the i-th protein level, b_{p_i} is the bias, i. e., the basal level of the i-th protein, and λ_{p_i} is the degradation rate of the i-th protein.

If we, instead of gene families, worked with genes coding for n_s individual subunits, then the first term on the right-hand side of (54.2) would read $\sum_j^{n_s}(\text{proportion of subunits}) \times m_j(t-\tau_{m_j})$ instead

of $m_i(t-\tau_{m_i})$. Second terms in (54.1) and (54.2) enable us to investigate the effect of drugs and other factors like neurotransmitters or hormones, which are known to influence gene–protein interactions.

We solve (54.1) and (54.2) numerically and interpret one iteration as 1 s of the real time. Equations (54.1) and (54.2) are the so-called delay differential equations (DDEs). DDEs are similar to ordinary differential equations, but their evolution involves past values of the state variable. The solution of delay differential equations therefore requires knowledge of not only the current state, but also of the state a certain time previously [54.55]. For DDEs we must provide not just the value of the solution at the initial point, but also the history, that is the solution at times prior to the initial point [54.56]. As of MATLAB 6.5 (Release 13), the DDEs solver **dde23** is part of the official MATLAB release.

54.3.2 Proteins and Neural Parameters

Let P_j denotes the j-th parameter of a model neuron. Let $p_j \in (0,1)$ be the normalized level of protein concentration obtained by the solution of (54.1) and (54.2) above. Then the value of parameter P_j is directly proportional to the concentration of the (functional) protein p_j, in such a way that

$$P_j(t) = p_j(t)\left(P_j^{\max} - P_j^{\min}\right) + P_j^{\min}\,, \qquad (54.3)$$

where $P_j^{\max}$ and $P_j^{\min}$ are maximal and minimal values of the j-th parameter, respectively. If $p_j \to 0$ then $P_j \to P_j^{\min}$, and if $p_j \to 1$ then $P_j \to P_j^{\max}$. Other, e.g., nonlinear relations between protein levels and parameter values are also possible. The linear relationship in (54.3) is justified by findings that protein complexes, which have clearly defined interactions between their subunits, have highly correlated levels with mRNA expression levels [54.57,58]. Subunits of the same protein complex show significant co-expression, both in terms of similarities of absolute mRNA levels and expression profiles, e.g., subunits of a complex have correlated patterns of expression over a time course [54.58]. This implies that there should be a correlation between mRNA and protein concentration, as these subunits have to be available in stoichiometric amounts for the complexes to function [54.57]. This is exactly the case of proteins in our model, which are receptors and ion channels, comprised of respective ratios of subunits. Equation (54.3) links the gene/protein dynamics to the dynamics of neural model. Values of neuronal parameters will not be constant anymore, but instead their values will depend on the levels of synthesized proteins [54.59, 60]. In such a way the system of (54.1) to (54.3) allows for investigation of how deleted or mutated genes can alter the activity of a neural network.

54.3.3 Thalamo-Cortical Model

We use the same spiking neural network as a thalamo-cortical model as we investigated in our previous studies of the cortical local field potential (LFP) and its dependence upon genes and proteins [54.43,44]. The cortical local field potential (LFP) is calculated at each time instant as the total sum of current membrane potentials of all neurons in the network model of cortex, i. e., $\Phi(t) = \Sigma u_i(t)$.

Spiking Neuron

The spiking model of the cortical neuron is an integrate-and-fire neuron [54.61, 62]. The total somatic postsynaptic potential (PSP) of neuron i is denoted as $u_i(t)$. We update u_i every millisecond (as opposed to the gene–protein dynamics that is updated every second). When $u_i(t)$ reaches the firing threshold $\vartheta_i(t)$, the neuron i fires, i. e., emits a spike (Fig. 54.4). The moment of the threshold $\vartheta_i(t)$ crossing from below defines the firing time t_i of an output spike. The value of $u_i(t)$ is the weighted sum of all synaptic PSPs, $\varepsilon_{ij}\left(t-t_j-\Delta_{ij}^{ax}\right)$, such that

$$u_i(t) = \sum_{j\in\Gamma_i}\sum_{t_j\in F_j} J_{ij}\varepsilon_{ij}\left(t-t_j-\Delta_{ij}^{ax}\right). \qquad (54.4)$$

The weight of synaptic connection from neuron j to neuron i is denoted by J_{ij}. It takes positive (negative) values for excitatory (inhibitory) connections, respectively. Δ_{ij}^{ax} is an axonal delay between neurons i and j, which linearly increases with Euclidean distance between neurons. The positive kernel expressing an individual postsynaptic potential (PSP) evoked on neuron i when a presynaptic neuron j from the pool Γ_i fires at time t_j has a double exponential form, i. e.,

$$\varepsilon_{ij}^{\text{type}}(s) = A^{\text{type}}\left[\exp\left(-\frac{s}{\tau_{\text{decay}}^{\text{type}}}\right) - \exp\left(-\frac{s}{\tau_{\text{rise}}^{\text{type}}}\right)\right], \qquad (54.5)$$

where $\tau_{\text{decay/rise}}^{\text{type}}$ are time constants of the fall and rise of an individual PSP, respectively, A is the PSP's amplitude, and *type* denotes one of the following: *fast_excitation, fast_inhibition, slow_excitation, and*

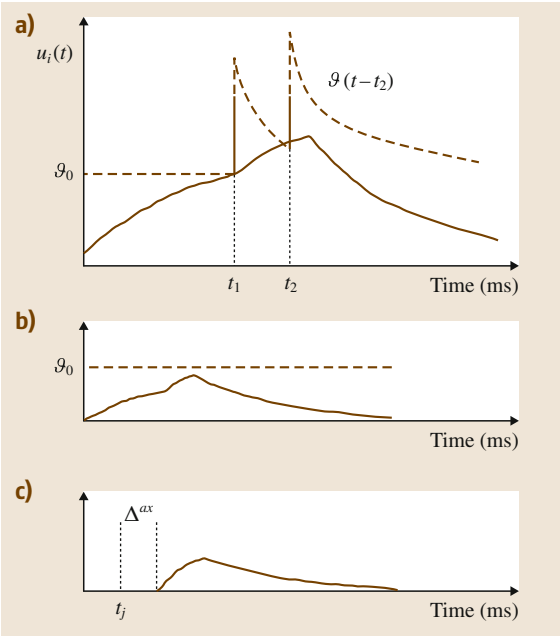

Fig. 54.4 **(a)** Suprathreshold summation of PSPs in the spiking neuron model. After each generation of postsynaptic spike there is a rise in the firing threshold that decays back to the resting value between the spikes. **(b)** Subthreshold summation of PSPs that does not lead to the generation of postsynaptic spike, but can still contribute to the generation of LFP. **(c)** PSP is generated after some delay of the presynaptic spike to travel from neuron j to neuron i

slow_inhibition. Fast excitation in excitatory synapses is mediated through the AMPA receptor-gated ion channels for sodium [54.18, 63]. Slow excitation in excitatory synapses is mediated through the NMDA receptor-gated ion channels for sodium and calcium [54.18,63]. Fast inhibition is mediated through the somatic $GABA_A$ receptor-gated ion channels for chloride, and slow inhibition is mostly mediated through the dendritic $GABA_B$ receptor-gated ion channels for potassium [54.16] as well as by the dendritic $GABA_A$ receptor-gated ion channels for chloride [54.17,21]. Immediately after firing the output spike at t_i, neuron's firing threshold $\vartheta_i(t)$ increases k-times and then returns to its resting value ϑ_0 in an exponential fashion

$$\vartheta_i(t-t_i) = k \times \vartheta_0 \exp\left(-\frac{t-t_i}{\tau^{\vartheta}_{\text{decay}}}\right) , \qquad (54.6)$$

where $\tau^{\vartheta}_{\text{decay}}$ is the time constant of the threshold decay. In such a way, absolute and relative refractory periods are modeled. Table 54.2 contains the values of neuron's parameters used in our simulations. These values were inspired by experimental and computational studies [54.18, 21, 64, 65] and were further adjusted by experimentation.

Table 54.2 List of neuronal parameters and initial values used in computer simulations

Neuron's parameters	Value range
Fast excitation: amplitude rise/decay time constants	0.5–3.0 1–5 ms/5–10 ms
Slow excitation: amplitude rise/decay time constants	0.5–4.0 10–20 ms/30–50 ms
Fast inhibition: amplitude rise/decay time constants	4–8 5–10 ms/20–30 ms
Slow inhibition: amplitude rise/decay time constants	5–10 20–80 ms/50–150 ms
Resting firing threshold, decay time constant/rise k	17–25 5–50 ms/1–5 fold

We assume that all three parameters in (54.5) for the fast excitation, i. e., amplitude, rise, and decay time constants are proportional according to (54.3) to the concentration of the protein called amino-methylisoxazole-propionic acid receptor or AMPAR in short. All three parameters describing slow excitation are proportional to the concentration of the N-methyl-D-aspartate acid receptor or NMDAR. All three parameters describing fast inhibition are proportional to the concentration of the gamma-aminobutyric acid (GABA) receptor A or $GABA_AR$ for short. The slow inhibition parameters are proportional to the levels of GABA receptor B (or $GABA_BR$). Concentration of the sodium voltage-gated channel (SCN) protein is inversely related to the firing threshold parameters, its resting value, and the decay constant. This inverse relationship is a trivial modification of the relation in (54.3). We could have made only the amplitudes dependent on the protein concentrations and we could have included more ion channel proteins to affect the firing threshold parameters. We do not claim particular assumptions above are the most appropriate. They do, however, serve our purpose to develop a model of SNN that has dynamically changing values of neuronal parameters that depend on levels of proteins which in turn depend on the dynamics of internal GPRN described by (54.1) and (54.2). Thus the values of parameters in Table 54.2 are initial values that change dynamically according to (54.3).

Spiking Neural Network

Figure 54.5 illustrates the architecture of our spiking neural network (SNN). Spiking neurons within the net-

Table 54.3 List of SNN parameters and values used in computer simulations

SNN Parameter	Value
Number of neurons	120
Proportion of inhibitory neurons	0.2
Probability of external input fiber firing	0.015
Peak/sigma of external input weight	5/1
Peak/sigma of lateral excitatory weights	10/4
Peak/sigma of lateral inhibitory weights	40/6
Probability of connection	0.5
Grid unit delay for excitatory/inhibitory spike propagation	1/2 ms

work that represents the cerebral cortex can be either excitatory or inhibitory. There can be as many as about 10–20% of inhibitory neurons positioned randomly on the rectangular grid of N neurons.

Lateral connections between neurons in the model cortex have weight values that decrease in strength with the distance from neuron i according to a Gaussian formula

$$J_{ij}(\mathrm{dist}(i,\,j)) = \frac{J_0^{\mathrm{exc/inh}}}{\sigma^{\mathrm{exc/inh}}} \exp\left(-\frac{\mathrm{dist}(i,\,j)^2}{\sigma^{\mathrm{exc/inh}^2}}\right) \quad (54.7)$$

while the connections are established at random with the probability equal to 0.5. The same distribution of weights and connectivity probability is applied to the feedforward connections from the input layer that represents the thalamus. External inputs from the input layer are added to the right-hand side of (54.4) in each time step. Each external input has its own weights $J_i^{\mathrm{ext\_input}}$ and the PSP evoked by the fast AMPAR-dependent excitation, i. e.,

$$u_i^{\mathrm{ext\_input}}(t) = J_i^{\mathrm{ext\_input}} \varepsilon_i^{\mathrm{fast\_excitation}}(t)\,. \quad (54.8)$$

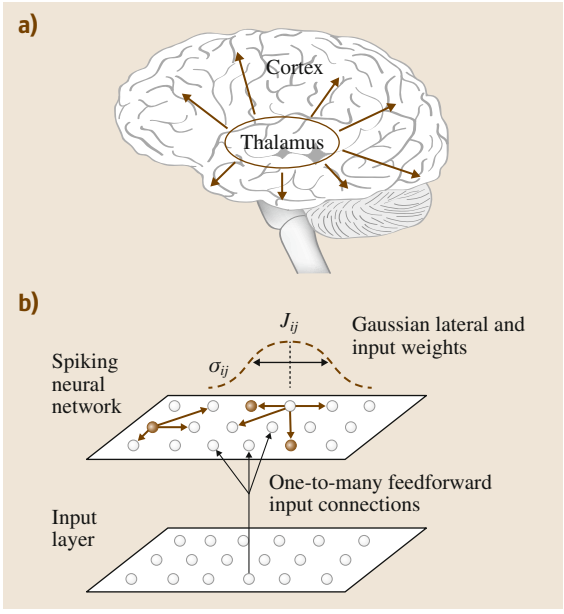

Fig. 54.5 **(a)** Simple neural network model of the thalamocortical (TC) system. **(b)** SNN represents the cortex and the input layer represents the thalamus. 20% of N neurons are inhibitory (*filled circles*). Units in both layers form a rectangular grid. The model does not have a feedback from the cortex to the thalamus

To stimulate the model cortex, we employed a uniformly random input with an average firing frequency of 15 Hz, since a tonic, low-frequency, nonperiodic and nonbursting firing of thalamocortical inputs with the frequency of 10–20 Hz is typical for the state of vigilance [54.66]. Table 54.3 contains the values of SNN parameters used in our simulations. Values of parameters like weight distributions and strengths and grid unit delays were adjusted by experimentation.

54.4 Dynamics of the Model

Figure 54.6 illustrates temporal evolution of variables at three levels, i. e., three dynamic systems that we combine into one integrated dynamic system – computational neurogenetic model.

The first dynamic system is the SNN, which similarly to biological neurons operates on the time scale of milliseconds (ms). Then we have changes in protein levels that lag behind the changes in gene expression/mRNA levels by the order of tens of minutes, even hours, due to the process of transcription, translation, and post-translational modification. Protein levels are directly related to parameters of neuronal signaling, like excitation and inhibition. Gene expression levels (expressed as mRNA levels) change slowly – on the order of tens of minutes, even hours.

54.4.1 Estimation of Parameters

Ideally we would know all the parameters in (54.1)–(54.3), that is, ideally we would know all the delays, bi-

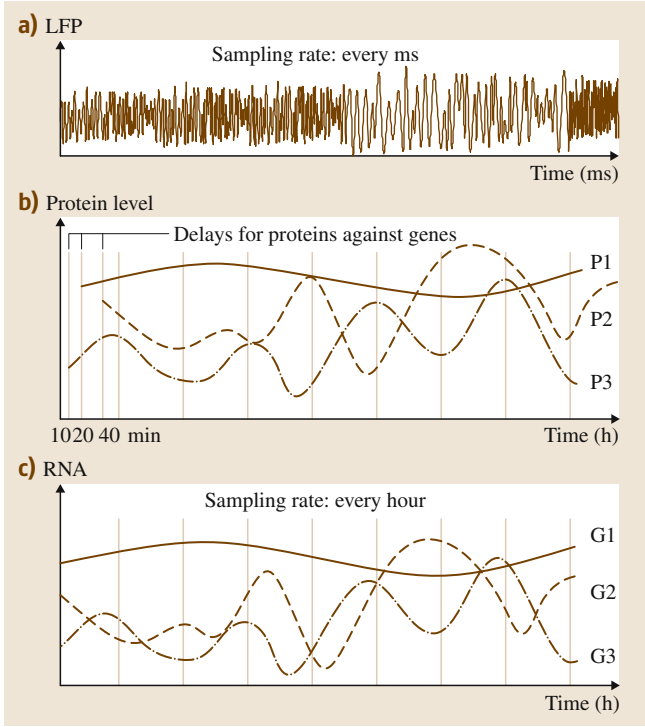

Fig. 54.6a–c Summary of three dynamic systems within one integrated dynamic system – computational neurogenetic model. **(a)** Local field potential (LFP) of SNN, **(b)** protein dynamics over time, **(c)** gene expression/mRNA dynamics over time

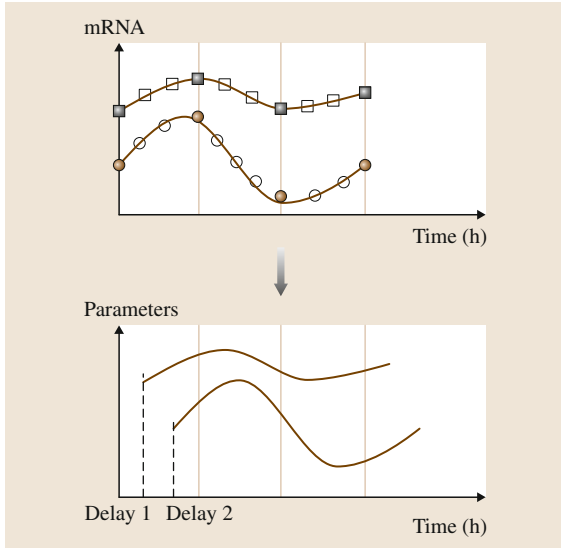

Fig. 54.7 From the measured and interpolated time evolution of mRNA levels, filled and empty symbols, respectively, we can derive the values of parameters for model neurons using (54.2) and (54.3)

ases, shapes of activation functions, amplitudes, degradation rates, and last but not least, the interaction matrix $\boldsymbol{W} = \{w_{ij}\}$. We could infer the coefficients of $\boldsymbol{W}$ from the time course of mRNAs by reverse engineering. To do so, we would have to proceed in the following steps:

1. Obtain gene expression data (mRNA levels) from the relevant neural system for discrete sampling periods.
2. Then use the interpolation technique (for instance the extended Kalman filter) to interpolate missing values for mRNA levels for intermediate time intervals. In such a way, we can obtain the values of all m_i for, let us say, every minute.
3. Then we need to calculate the levels of proteins according to (54.2) to estimate the values of neuronal parameters according to (54.3), see Fig. 54.7.

Let us now discuss these steps in more detail. The first step, i. e., the interpolation, would enable us to work with the values of mRNAs and consequently parameter values in one-minute intervals. We can assume the values of neuronal parameters being constant during these short intervals between interpolated values. Different methods can be used for data interpolation, for instance the Kalman filter [54.67, 68], evolutionary optimization [54.69], state space equations [54.70], etc. Then the biggest challenge is to estimate the delays from initiation of transcription of the gene families till the end of synthesis of relevant proteins in the gene–protein regulatory network, i. e., τ_{m_i}'s for (54.2). We need these delays for updating neuronal parameters to simulate SNN (or any other ANN model).

Proper updating of neuronal parameters is crucial for explaining changes in the SNN output – why they occur and when. We can make rough qualified estimates of these delays using the information of the length of the relevant proteins and the time, which is needed for their genes transcription and the subsequent protein translation [54.45] and posttranslational modifications [54.46]. After all this, the final computational challenge remains: the simulation of SNN activity in real time.

54.4.2 Simulation Plan

Another option is that instead of simulating the SNN for the whole time of evolving gene–protein dynamics, we can perform the simulations of SNN only at random or interesting time points of the gene–protein dynamics, as

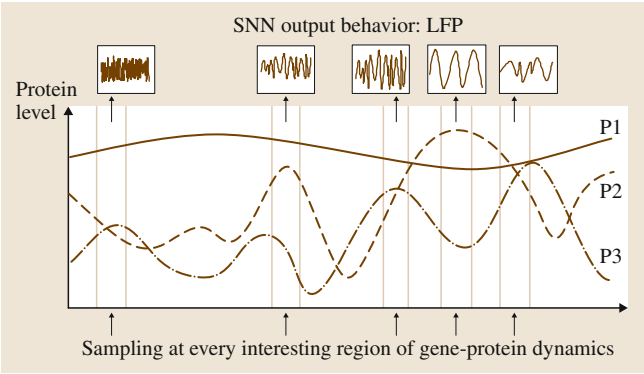

Fig. 54.8 Sampling the SNN output at interesting time intervals based on some heuristics. LFP means local field potential ▶

is illustrated in Fig. 54.8. For these random or interesting time points, the simulations of SNN will last only for some minutes of real time. Interesting intervals for sampling the SNN output can be based on some kind of heuristics – for instance based on the knowledge that at that particular time something has happened – for instance, there was a seizure. Otherwise this sampling can occur at intervals where the parameters have their extreme values, at intersections of values, etc.

54.5 Results of Computer Simulations

54.5.1 Dynamics of the Gene–Protein Regulatory Network

In order to illustrate the approach described above, we provide an example of an artificially created dynamic system described by (54.1)–(54.3). We have omitted the terms for external factors from both equations. Thus, we have numerically solved (54.1)–(54.3) (minus external factors terms) for several randomly generated interaction matrices $\boldsymbol{W}$s, with random coefficients $w_{ij} \in (-1, 1)$ and with randomly generated delays τ_{p_j}, $\tau_{m_i} \in (0\,\text{min}, 60\,\text{min})$. Other parameters had these values: $\sigma_{m_i}(x) = \sigma_{p_i}(x) = \tanh(x)$ for each i, $A_{m_i} = A_{p_i} = 0.01$ for each i, $b_{m_i} = b_{p_i} = 0.5$ for each i, and $\lambda_{m_i} = \lambda_{p_i} = 0.001$ for each i. These constants were chosen in such a way that the oscillations in gene and protein dynamics were on the orders of 1–2 or more hours [54.71]. The values of mRNAs and proteins were normalized to the interval $(0, 1)$. The total number of genes was $n = 10$, where five genes were directly related to the signal processing parameters and five genes were not. These five hypothetical genes directly affecting values of neural parameters were: AMPAR, NMDAR, GABAAR, GABABR, and SCN. For better clarity, we present only the curves for the five genes that are directly related to parameters. Initial conditions are always the same unless otherwise stated and that is $m_i(0) = 0.5$ and $p_i(0) = 0.5$ for all i.

In Fig. 54.9 we illustrate the effect of different delays upon the steady state gene dynamics for the same random $\boldsymbol{W}$ and the same initial conditions. The interval for numerical solving of (54.1) and (54.2) was equal to 1 s. We can see that delays can completely change

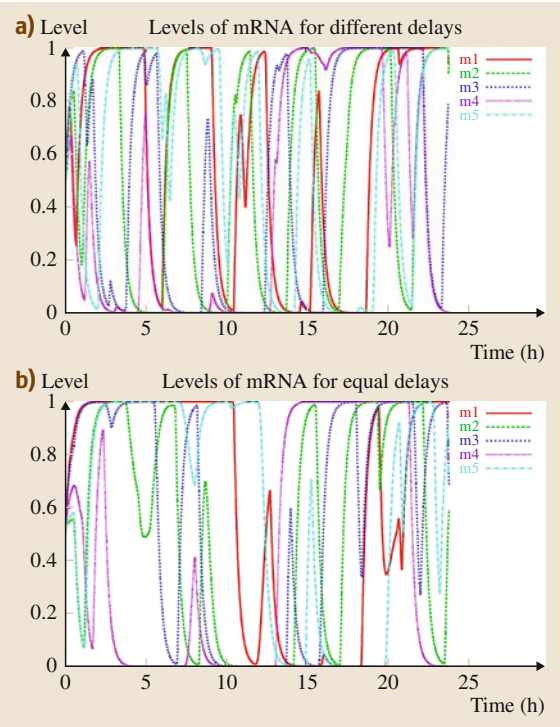

Fig. 54.9a,b Effect of different delays upon the gene dynamics for the same GPRN interaction matrix $\boldsymbol{W}$ and the same initial conditions: **(a)** the delays are randomly generated from the interval 0–60 min, **(b)** all delays are equal to 30 min ▶

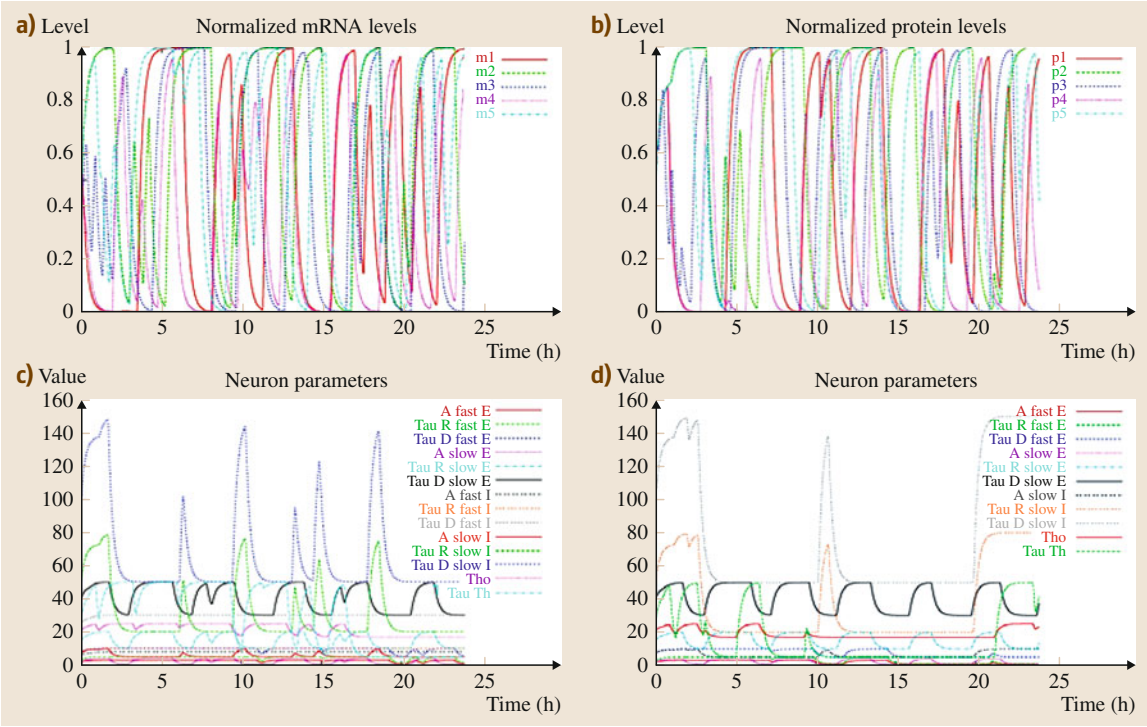

Fig. 54.10a–d A typical example of **(a)** mRNA dynamics (54.1), **(b)** protein dynamics (54.2), and **(c)** parameter dynamics (54.3) for one randomly generated GPRN interaction matrix $\boldsymbol{W}$ and one set of randomly generated delays. All delays are different and randomly generated from the interval (0 min, 60 min).**(d)** Temporal dynamics of the neuron's parameter values after the knock out of hypothetical genes for $GABA_AR$. Parameters related to fast inhibition are missing entirely and the other ones have changed their time course

the time course of mRNAs for the same values of other parameters. Therefore, in simulations of real experiments it would be very important to estimate the delays carefully.

In the next Fig. 54.10 we present a typical example of mRNA dynamics (54.1), protein dynamics (54.2), and related neuronal parameter dynamics for one of the randomly generated gene–protein regulatory matrices $\boldsymbol{W}$ and a set of randomly generated delays. All delays are different and randomly generated from the interval (0 min, 60 min). The time scale is in hours, and the whole simulation illustrates the gene and protein levels over 24 h. The update interval for the gene–protein dynamics was 1 s. We can see in Fig. 54.10a,b that the protein dynamics is essentially copying the gene dynamics, however with corresponding delays. The typical steady state of our model system resembles chaotic or quasi-periodic behavior. Constant or periodic steady states are rare.

54.5.2 Dynamics of GPRN After Gene Knock Out

In our artificial GPRN, we can *delete* or *mutate* genes one after another, and in various combinations, and observe the effect upon the parameter and consequently upon the SNN dynamics. In the model, we can manipulate also the genes that are not directly related to neuronal parameters, but that influence them through regulatory interactions $\boldsymbol{W}$. In such a way, a computational model can aid an experimental search for various genetic conditions. For illustration, we will *knock out* one hypothetical gene, let us say that one responsible for $GABA_A$ receptors mediating fast inhibition in our model. $GABA_A$ receptor mRNA and protein levels as well as related parameters are all set to zero for the whole time of the simulation. The resulting parameter dynamics after $GABA_AR$ gene deletion is illustrated in Fig. 54.10d. All the coefficients of the interaction ma-

trix $\boldsymbol{W}$ are the same as for the dynamics illustrated in Fig. 54.10a–c, except of course all the links from knock out gene $GABA_AR$ are missing. We can see in Fig. 54.10d even with the naked eye that for the same initial conditions, the parameter dynamics governed by genes–protein network has changed compared to the complete GPRN. The curves corresponding to parameters related to fast inhibition are missing entirely, timing of others has changed. The prominent peaks in both graphs c and d belong to the decay constant of slow inhibition. After the knock out of $GABA_AR$ four peaks are missing in the dynamics of this slow inhibition parameter and a new peak appears after 20 h. The same holds for other parameters of slow inhibition. Although they have different values, they follow the same time courses because that is the time course of the concentration of NMDAR. We can conclude, not surprisingly, that the temporal evolution of all neural parameters has changed more or less as a consequence of the knock out of the hypothetical gene for $GABA_AR$.

54.5.3 Dynamics of the Cortex

The question arises now what the spiking activity of the SNN is like. Figure 54.11 illustrates the spiking of SNN over 1 min at some arbitrary time point of parameter dynamics of parameters illustrated in Fig. 54.10c. When the small artificial genome is complete, many random gene interaction matrices actually lead to an asynchronous spiking of SNN with very low frequencies and low spike count, like the one illustrated in Fig. 54.11.

54.5.4 Dynamics of the Cortex After Gene Knock Out

Now, we are interested in the effect of the gene knock out upon the SNN local field potential and spiking activity. We performed the SNN simulations and the LFP activity analysis for the same time intervals as in the case of a complete GPRN. Interestingly, most of the time, the spiking activity of SNN was low and asynchronous, like in the *normal* case illustrated in Fig. 54.11, in spite of the fact that the $GABA_AR$ gene and thus the fast inhibition were entirely missing. It seems that for this particular interaction matrix $\boldsymbol{W}$ there was a compensation for the missing fast inhibition most of the time. However, sometimes all the neurons in the SNN spontaneously synchronized. This behavior is illustrated in Fig. 54.12. Such behavior is reminiscent of a spontaneous epileptiform activity that spontaneously

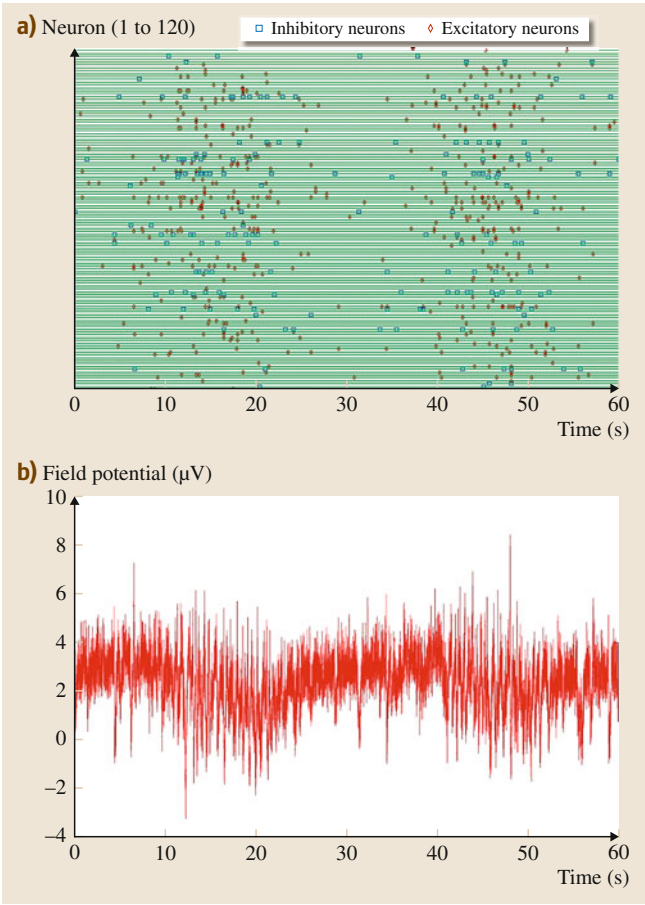

Fig. 54.11a,b Illustration of the output behavior of SNN for the complete artificial genome: **(a)** The spiking behavior. The x-axis is time and the y-axis is the index of a neuron. The spikes of excitatory neurons are marked by *red blobs* and the spikes of inhibitory neurons are marked by the *blue blobs*. Neurons spike on average with very low frequency of 0–0.5 Hz. At any millisecond interval only 0–4 neurons emit a spike. **(b)** The *graph* shows the corresponding local field potential (LFP), which is the sum of all membrane potentials of all neurons

arises and then ceases again. The SNN entered the synchronized state and left it spontaneously based on the underlying parameter dynamics. Most of the time however, the spiking was asynchronous like the one illustrated in Fig. 54.11, in spite of the fact that the gene for $GABA_AR$ was missing from the artificial genome.

To summarize, the observed behavior before and after the simulated knock out of the hypothetical gene for $GABA_AR$ from our artificial gene–protein regulatory network resulted from several randomly generated

interaction matrices $\boldsymbol{W}$. Most of the randomly generated regulatory matrices either produced no spiking in the SNN or the neurons were synchronized all the time. We did not perform any optimization of the interaction matrix $\boldsymbol{W}$ like we did, for instance, in our previous work by means of an evolutionary algorithm where the fitness function was particular spectrum of LFP or EEG [54.43,44]. Rather, we adopted an exploratory approach of investigation of many randomly generated interaction matrices out of which we kept those that generated interesting dynamics. This naïve brute force approach served us to explore the potential application of computational neurogenetic model in relation to gene knock-out experiments.

54.6 Discussion and Future Directions

With the advancement of molecular research technologies more and more data and information will be made available about the genetic basis of neuronal functions and genetically based epilepsies and other brain genetic diseases. This information will then be utilized for the models of brain functions and diseases that include models of gene and protein interaction within neurons. Although the data are not yet available, we have started to conceive a new computational methodology that will be able to incorporate such knowledge into the existing models of neurons and neural networks. This new approach integrates knowledge from computer and information science, neuroscience, and molecular genetics. We call it computational neurogenetic modeling [54.43]. In this chapter we describe this novel computational approach to brain neural network modeling which integrates dynamic gene–protein networks with a neural network model. The bridging system is the protein network, in which individual proteins that are coded for by genes are related to neuronal parameters. Interaction of genes and proteins in model neurons thus affects the dynamics of the whole neural network through neuronal parameters, which are no longer constant, but change as a function of gene expression. For simulation of real experiments we would need real gene expression data to infer the parameters of GPRN. Then, through optimization of the gene interaction network, initial gene/protein expression values and neural parameters, particular target states of the neural network operation can be achieved. At present however, no such data are available. Therefore we have adopted an exploratory approach to demonstrate this new computational methodology by means of a simple neurogenetic model of a spiking neural network which generates LFP and we have shown some interesting behavior of this simple model.

Recently, *Thomas* et al. [54.72] adopted a kind of reverse approach. Using a computational model of dentate gyrus with mossy fiber sprouting they addressed these three questions: (1) What voltage-gated ion channels have the biggest influence on network excitability? (2) What changes in their electrophysiological properties have the biggest influence on network excitability? (3) What is the magnitude of these changes that leads to epileptiform activity? They call this approach a *genetic sensitivity* analysis to predict which genes are best positioned to increase risk as well as to predict *functionally* how variants in these genes might increase network excitability. Based on computer simulations they predicted that variants in sodium and delayed rectifier channels are likely to confer risk for development of epilepsy. This prediction is consistent with findings that mutations in genes coding these channels can cause generalized epilepsies (see, e.g., Table 54.1), although generalized epilepsy syndromes predominantly involve cortical and thalamic networks (like we simulated in this chapter albeit with only feedforward connectivity) and not dentate gyrus. Notable is the used model of the neural network. *Thomas* et al. [54.72] used a model of the dentate gyrus that contains morphologically realistic models of granule cells, and other excitatory and inhibitory neurons developed using the software NEURON [54.73, 74]. Neuron models had between 9 and 17 compartments describing the actual dendritic arborization and realistic conductances including the fast sodium and potassium channels that directly form the action potential, an A current, L-, N-, and T-type calcium channels, hyperpolarization-activated, cyclic nucleotide-gated (HCN) current, and slow-voltage and calcium-gated potassium channels. Similarly, a detailed neural network model of the relevant brain areas in connection with computational neurogenetic modeling will allow us to ask more detailed questions and simulate more detailed situations than we have shown in this chapter. At the time of writing of this chapter more than 600 of such detailed computational models were publicly available at the ModelDB website of the NEURON simulation environment [54.75].

54.6.1 Q and A for Neurogenetic Modeling

Computational neurogenetic modeling is a new area of research that has many open questions, for example:

1. *Which real neuronal parameters are to be included in an ANN model and how to link them to activities of genes/proteins?*
   In our model presented in this chapter, we have chosen those parameters that are relevant to neuronal excitation and inhibition as our goal was to model LFP and the consequence of gene knock out (or mutation) upon the changes in LFP that would resemble epileptiform activity. Thus, the general answer to this question would be to include those parameters that are relevant for the phenomenon modeled. We have linked the chosen parameters to the levels of proteins via (54.3). This linkage is based on the assumption that the magnitude of excitation/inhibition is proportional to the concentration of corresponding receptors for excitatory/inhibitory neurotransmitters, respectively. Or in other words, this assumption means that if the gene expression for particular receptor is increased/decreased, then there is probably an increased/decreased demand for it in the cell due to changes in synaptic transmission or due to effects of other genes. However, in addition to this relationship a more sophisticated relation is possible to model. Different variants of relevant genes are linked with variations in receptor or ion channels functions and that can be taken into account as well.
2. *Which genes/proteins are to be included in the model and how to represent the gene interaction over time within each neuron?*
   In our simple model we worked with the gene families that code for subunits of receptors or ion channels. We have also suggested how to extend the model to include individual genes. In addition to the genes that are directly related to neuronal parameters, there are also many other genes that influence them. These other genes can be found in the available literature and bioinformatics databases. For instance, the Ingenuity Pathway Analysis (IPA) system can be used to investigate interaction-based relationships between the genes and proteins based on their own Ingenuity Knowledge Base [54.76]. Then the choice of a particular computational model of gene–protein interaction should depend on the information that is available about the modeled system. There are many available theoretical models of gene–protein interaction networks, e.g., differential equations, stochastic models, weight matrices, Boolean models, etc.
3. *How can we integrate in time the activity of genes, proteins, and neurons in an ANN model, as it is known that neurons spike in millisecond intervals and the process of gene transcription and translation into proteins takes minutes or even hours?*
   This is really a computational issue that depends on the computational power available. Ideally one would simulate at the same time the internal gene–protein regulatory network and its effect upon neural parameters in the real time. An alternative solution is to run the GRN dynamics separately, store the results and feed the values of protein levels to the neural model only for some interesting intervals of gene–protein dynamics. We have adopted this approach in this chapter. As we did not know which periods of gene–protein dynamics were interesting, we just picked several intervals at random. This approach has the disadvantage that some interesting events in the dynamics of the model can be easily missed.
4. *How can we integrate internal and external variables in a CNGM (e.g., genes and neuronal parameters with external signals acting on the brain)?*
   The basis for this integration can be the second terms in (54.1) and (54.2). These terms express the effect of chemical agents be it drugs or upon the levels of mRNA and proteins. Our model can, in principle, be extended to include also the activity-dependent changes in neural parameters [54.42] and synaptic plasticity [54.20].
5. *How can we measure brain activity and the CNGM activity in order to validate the model?*
   Although our neural network is a model of LFP, since EEG is the sum of many LFPs [54.77], the EEG record like in Fig. 54.1 can serve as a validation of the model of epilepsy. For instance, we can see in Fig. 54.1 that there are about five epileptic slow-wave discharges starting at second 10, which then spontaneously cease. It seems another series starts between 20 and 25 s of the EEG record but the record suddenly ends. If we compare this behavior with the model spiking in Fig. 54.12, we can see it is, indeed, very similar in that each time there is an epileptiform behavior there are only few waves of global synchronization of neurons that spontaneously emerge and then cease and there is an inter-ictal interval of 20 s. Duration of periods between seizures is, however, highly variable in our

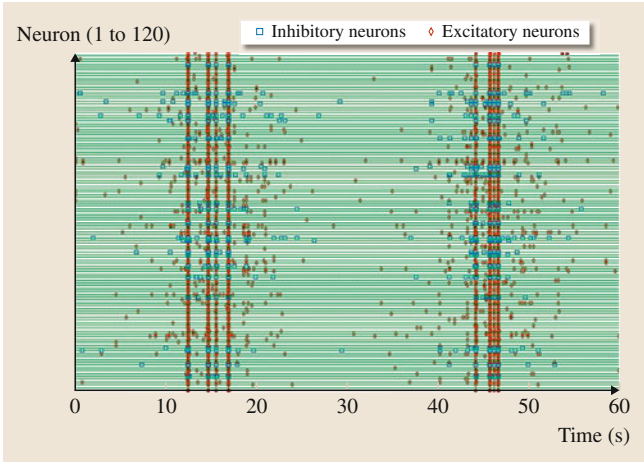

Fig. 54.12 After the knock out of the gene coding for $GABA_AR$, the SNN behavior was reminiscent of a spontaneous intra-ictal and inter-ictal activity. This is one particular illustration when the seizure-like synchronizations occurred in close succession within 1 min of simulated time. In general intervals between seizure-like activities varied widely

model and depends on the underlying GPRN dynamics that is relatively slow compared to neural dynamics.

6. *What is the effect of connectivity? How does it interact with the effects of GPRN?*
   In each SNN simulation, the particular connectivity was different, albeit constructed according to the same statistics. It would be interesting to investigate whether connectivity can compensate for gene defects, or vice versa, or whether connectivity can lead to pathology even when the genome is complete with no mutations. We would need more information on variations of interneuronal connectivity between individuals and between the healthy subjects and subjects with epilepsy to be able to carry out this investigation.
7. *What useful information can be derived from CNGM?*
   What happens if the nucleotide sequence of the gene encoding the protein is altered or deleted? Such changes in the DNA sequence, called mutations, can lead to the loss of the encoded protein or to a change in its structure, thereby altering its function. For instance, gene mutations may decrease or increase the activity of a given gene product or they may result in setting a new activity of the gene product [54.78]. Even when only one gene is mutated, the expression of other genes in the whole GRN may be more or less affected. Sometimes a gene mutation matters and sometimes it does not. Everything depends on the function of its product and on its interactions with other genes in the GRN. Moreover, there can be mutations in the DNA sequence outside the gene region that correspond to the various gene expression regulation sites. While mutation of an activator-binding site leads to decreased expression of the linked gene, mutation of a repressor-binding site leads to increased expression of the gene. In our simple model we simulated the gene knock out in such a way, that the expression of the corresponding gene was set to zero and all the interactions to and from this gene were set to zero. In the case of the mutated gene, these interactions may remain intact and just the expression level can be modified, either increased or decreased. This will have an effect upon other genes in the network, and we can observe how the dynamics of the neural network changes. Thus, the computational neurogenetic approach has great potential in modeling gene dynamics and its changes due to DNA mutations and the consequences upon the neural dynamics.

These and many more questions remain to be addressed in the future. Although we are speaking about brain diseases and functions, having in mind mammals and higher vertebrates, the approach suggested in this chapter is applicable also to simpler organisms to aid the explanation of the genetic basis of their behaviors. Another system that can be used to validate our approach could be brain slices taken from normal and genetically modified brains.

54.6.2 Hypothesis

It is interesting to note that in our illustrative example that, in spite of the fact that the artificial gene–protein network has been altered due to one gene knock out, the dynamics of SNN in terms of spiking activity was most of the time very similar to the result obtained with the complete GPRN (Fig. 54.12). However, from time to time the neurons spontaneously temporarily synchronized their spiking as illustrated in Fig. 54.12. Thus, the knock out of a hypothetical gene for fast inhibition in our artificial genome has led to an epileptiform activity. In our model, the fluctuations in the values of neuronal parameters led to spontaneous development of seizure-like global synchronizations. These very same fluctuations also led to termination of the seizure-like neural activity and maintenance of the inter-

ictal normal periods of activity. Our hypothesis does not rule out other mechanisms of seizure development, maintenance, and cessation, like for instance activity-dependent changes in neural parameters [54.42] and/or synaptic entraining [54.20], or other mechanism(s) like the processes in the thalamocortical recurrent loop, which we did not include in our model at all [54.34]. Based on our model, however, we would like to suggest a hypothesis that the parameter changes due to the gene–protein dynamics should also be included as a serious factor that determines transitions in neural dynamics, especially when the cause of disease is known to be genetic. This hypothesis can be tested, for instance, in slices or neuronal cultures from the wild type and gene knock out mice.

54.6.3 Robustness of Gene Regulatory Networks

Even in the presence of a mutated gene in the genome that is known to cause the brain disease, the neurons can still function normally provided a certain pattern of interaction between the genes is maintained [54.79]. It seems the expression regulation between genes is so robust that it can compensate, at least to some extent, for mutations in the genes. In fact, in our computer experiments, we observed that several different gene dynamics, i. e., several different regulatory matrices $\boldsymbol{W}$s can lead to very similar SNN LFPs and spiking activities. This observation relates to the hot topic of robustness versus evolvability of gene regulatory networks. It seems that our system manifests a certain robustness. We do not mean the robustness against noise or stochasticity in gene expression because our model system is fully deterministic. What we have discovered in our exploratory simulations is a certain robustness with respect to different regulatory interactions between the same set of genes leading to the same phenotype expressed as the spiking activity of the model SNN.

Biochemical parameters that determine the behavior of cellular systems – from proteins to genome-scale regulatory networks – change continually. These changes have two principal sources. One of them is genetic and consists of mutations. The other is not genetic and is related to noise internal to the organism and/or induced by environmental change. Much of the noise consists of stochastic variation in gene expression and expression regulation. Such noise makes all biochemical parameters affecting the cell's behavior appear to fluctuate randomly. Environmental change, such as a change in temperature, salinity, or nutrient availability, can similarly affect many parameters at once in random manner. Such observations suggest that biological circuits are not fine-tuned to exercise their functions only for precise values of their biochemical parameters. Many biochemical parameters driving circuit behavior vary extensively and are thus not fine-tuned. Instead, biological circuits including gene regulatory networks must be able to function under a range of different parameters. In other words, they must be robust to parameter change. Current genetic and modeling research tries to elucidate the robustness of gene regulatory networks with respect to transcriptional mechanisms that cause robust versus stochastic gene expression and their relationship to phenotypic robustness and variability [54.80, 81].

In addition, it seems that organisms are robust to a great variety of genetic changes. *Aldana* et al. [54.82] addressed a problem of robustness and evolvability of the attractor landscape of genetic regulatory network models under the process of gene duplication followed by divergence. They showed that an intrinsic property of this kind of network is that, after the divergence of the parent and duplicate genes, with a high probability the previous phenotypes, encoded in the attractor landscape of the network, are preserved and new ones might appear. The above is true in a variety of network topologies and even for the case of extreme divergence in which the duplicate gene bears almost no relation with its parent. Their results indicate that networks operating close to the so-called *critical regime* exhibit the maximum robustness and evolvability simultaneously.

Ciliberti et al. (2007) argue that the topology of gene regulatory networks, that is who-interacts-with-whom, is the key to understanding their robustness to both mutations and noise [54.83]. The latter authors performed theoretical and computational investigation for a weight matrix model of transcriptional regulation networks, in which they explored millions of different network topologies. Topology is synonymous with the *structure* of the matrix $\boldsymbol{W}$, where each of $\boldsymbol{W}$'s nonzero entries corresponds to one regulatory interaction among the network's genes. Changes in topology correspond to the loss of a regulatory interaction, or to the appearance of a new regulatory interaction that was previously absent. The robust feature is the network's equilibrium gene expression pattern. Robustness to mutations corresponds to robustness of changes in regulatory interactions, either as a change in network topology, or as a change in the strength of regulatory interaction. Robustness to noise corresponds to robustness of equilibrium gene expression pattern to random changes in gene expression

patterns. First, they showed that robustness to mutations and noise were correlated in these networks. They showed a skewed distribution, with a very small number of networks being vastly more robust than the rest. More importantly, they also showed that highly robust topologies can evolve from topologies with low robustness through gradual topological changes. Thus, they argue robustness is an evolvable property and that evolvability of robust networks may be a general principle of evolutionary process. This result is general and thus applies to gene regulatory networks in the brain as well. It is congruent with the results of our exploratory simulations of spiking behavior of model SNN whose neuronal parameters of excitation and inhibition are dynamically varied due to the dynamics of internal gene–protein interaction network.

References

54.1 H. Lodish, A. Berk, S.L. Zipursky, P. Matsudaira, D. Baltimore, J. Darnell: *Molecular Cell Biology*, 5th edn. (Freeman, New York 2000), Chap. 10: Regulation of transcription initiation, pp. 341–403

54.2 L. Benuskova, N. Kasabov: *Computational Neurogenetic Modeling* (Springer, New York 2007)

54.3 H. Meinhardt: Different strategies for midline formation in bilaterians, Nat. Rev. Neurosci. **5**, 502–510 (2004)

54.4 M. Kerszberg, J.-P. Changeux: Molecular models of early neural development. In: *Modeling Neural Development*, ed. by A. van Ooyen (MIT Press, Cambridge 2003) pp. 1–26

54.5 G. Marnellos, E.D. Mjolsness: Gene network models and neural development. In: *Modeling Neural Development*, ed. by A. van Ooyen (MIT Press, Cambridge 2003) pp. 27–48

54.6 C. Lee, K. Bae, I. Edery: The Drosophila CLOCK protein undergoes daily rhythms in abundance, phosphorylation, and interactions with the PER-TIM complex, Neuron **21**, 857–867 (1998)

54.7 V. Suri, A. Lanjuin, M. Rosbash: TIMELESS-dependent positive and negative autoregulation in the Drosophila circadian clock, EMBO J. **18**, 675–686 (1999)

54.8 P. Smolen, P.E. Hardin, B.S. Lo, D.A. Baxter, J.H. Byrne: Simulation of Drosophila circadian oscillations, mutations, and light responses by a model with VRI, PDP-1, and CLK, Biophys. J. **86**, 2786–2802 (2004)

54.9 National Center for Biotechnology Information: The nervous system. In: *Genes and Disease* (National Center for Biotechnology Information, Bethesda 2011), available online at http://www.ncbi.nlm.nih.gov/books/NBK22197/ (last accessed 3 May 2013)

54.10 M.E. Hasselmo: Neuromodulation and the hippocampus: Memory function and dysfunction in a network simulation. In: *Disorder of Brain, Behavior and Cognition: The Neurocomputational Perspective*, ed. by J.A. Regia, E. Ruppin, D. Glanzman (Elsevier, Amsterdam 1999) pp. 3–18

54.11 D. Horn, N. Levy, E. Ruppin: Multimodular networks and semantic memory impairments. In: *Disorders of Brain, Behavior and Cognition: The Neurocomputational Perspective*, ed. by J.A. Regia, E. Ruppin, D. Glanzman (Elsevier, Amsterdam 1999) pp. 68–72

54.12 E.D. Menschik, L.H. Finkel: Cholinergic neuromodulation and Alzheimer's disease: From single cells to network simulation. In: *Disorders of Brain, Behavior and Cognition: The Neurocomputational Perspective*, ed. by J.A. Reggia, E. Ruppin, D. Glanzman (Elsevier, Amsterdam 1999) pp. 19–45

54.13 H.P. Goodkin: The founding of the American Epilepsy Society: 1936–1971, Epilepsia **48**(1), 15–22 (2007)

54.14 O. Devinsky: Diagnosis and treatment of temporal lobe epilepsy, Rev. Neurol. Dis. **1**(1), 2–9 (2004)

54.15 Y. Ben Ari, R. Cossart: Kainate, a double agent that generates seizures: Two decades of progress, Trends Neurosci. **23**, 580–587 (2000)

54.16 B.W. Connors, R.C. Malenka, L.R. Silva: Two inhibitory postsynaptic potentials, and $GABA_A$ and $GABA_B$ receptor-mediated responses in neocortex of rat and cat, J. Physiol. **406**, 443–468 (1988)

54.17 J.A. White, M.I. Banks, R.A. Pearce, N.J. Kopell: Networks of interneurons with fast and slow g-aminobutyric acid type A ($GABA_A$) kinetics provide substrate for mixed gamma-theta rhythm, Proc. Natl. Acad. Sci. USA **97**, 8128–8133 (2000)

54.18 A. Destexhe: Spike-and-wave oscillations based on the properties of $GABA_B$ receptors, J. Neurosci. **18**, 9099–9111 (1998)

54.19 R.D. Traub, R. Miles, R.K. Wong: Models of synchronized hippocampal bursts in the presence of inhibition. I. Single population events, J. Neurophysiol. **58**(4), 739–751 (1987)

54.20 B. Biswal, C. Dasgupta: Neural network model for apparent deterministic chaos in spontaneously bursting hippocampal slices, Phys. Rev. Lett. **88**, 88–102 (2002)

54.21 F. Wendling, F. Bartolomei, J.J. Bellanger, P. Chauvel: Epileptic fast activity can be explained by a model of impaired GABAergic dendritic inhibition, Eur. J. Neurosci. **15**, 1499–1508 (2002)

54.22 P. Kudela, P.J. Franaszcuk, G.K. Bergey: Changing excitation and inhibition in simulated neural networks: Effects on induced bursting behavior, Biol. Cybern. **88**, 276–285 (2003)

54.23 M.C. Picot, M. Baldy-Moulinier, J.P. Daurès, P. Dujols, A. Crespel: The prevalence of epilepsy and pharmacoresistant epilepsy in adults: A population-based study in a Western European country, Epilepsia **49**, 1230–1238 (2008)

54.24 L. Wittner, L. Eross, S. Czirjak, P. Halasz, T.F. Freund, Z. Magloczky: Surviving CA1 pyramidal cells receive intact perisomatic inhibitory input in the human epileptic hippocampus, Brain **128**, 138–152 (2005)

54.25 J. DeFelipe: Types of neurons, synaptic connections and chemical characteristics of cells immunoreactive for calbindin-D28K, parvalbumin and calretinin in the neocortex, J. Chem. Neuroanat. **14**, 1–19 (1997)

54.26 B. Schwaller, I.V. Tetko, P. Tandon, D.C. Silveira, M. Vreugdenhil, T. Henzi, M.-C. Potier, M.R. Celio, A.E.P. Villa: Parvalbumin deficiency affects network properties resulting in increased susceptibility to epileptic seizures, Mol. Cell. Neurosci. **25**, 650–663 (2004)

54.27 A.E.P. Villa, Y. Asai, I.V. Tetko, B. Pardo, M.R. Celio, B. Schwaller: Cross-channel coupling of neuronal activity in parvalbumin-deficient mice susceptible to epileptic seizures, Epilepsia **46**(6), 359 (2005)

54.28 M. Vreugdenhil, J.G.R. Jefferys, M.R. Celio, B. Schwaller: Parvalbumin-deficiency facilitates repetitive IPSCs and related inhibition-based gamma oscillations in the hippocampus, J. Neurophysiol. **89**, 1414–1423 (2003)

54.29 L. Benuskova, N. Kasabov: Modeling brain dynamics using computational neurogenetic approach, Cogn. Neurodyn. **2**(4), 319–334 (2008)

54.30 R.M. Gardiner: Genetic basis of human epilepsies, Epilepsy Res. **36**, 91–95 (1999)

54.31 V. Crunelli, N. Leresche: Childhood absence epilepsy: Genes, channels, neurons and networks, Nat. Rev. Neurosci. **3**, 371–382 (2002)

54.32 C. Marini, L.A. Harkin, R.H. Wallace, J.C. Mulley, I.E. Scheffer, S.F. Berkovic: Childhood absence epilepsy and febrile seizures: A family with a $GABA_A$ receptor mutation, Brain **126**, 230–240 (2003)

54.33 H.K.M. Meeren, J.P.M. Pijn, E.L.J.M. van Luijtelaar, A.M.L. Coenen, F.H.L. da Silva: Cortical focus drives widespread corticothalamic networks during spontaneous absence seizures in rats, J. Neurosci. **22**, 1480–1495 (2002)

54.34 A. Destexhe, D.A. McCormick, T.J. Sejnowski: Thalamic and thalamocortical mechanisms underlying 3 Hz spike-and-wave discharges. In: *Disorders of Brain, Behavior and Cognition: The Neurocomputational Perspective*, ed. by J.A. Reggia, E. Ruppin, D. Glanzman (Elsevier Science, Amsterdam 1999) pp. 289–307

54.35 W.W. Lytton, D. Contreras, A. Destexhe, M. Steriade: Dynamic interactions determine partial thalamic quiescence in a computer network model of spike-and-wave seizures, J. Neurophysiol. **77**, 1679–1696 (1997)

54.36 R.M. Gardiner: Genetic basis of human epilepsies, Epilepsy Res. **36**, 91–95 (1999)

54.37 M.H. Meisler, J. Kearney, R. Ottman, A. Escayg: Identification of epilepsy genes in human and mouse, Annu. Rev. Genet. **35**, 567–588 (2001)

54.38 O.K. Steinlein: Genetic mechanisms that underlie epilepsy, Nat. Rev. Neurosci. **5**, 400–408 (2004)

54.39 A.L. George: Inherited channelopathies associated with epilepsy, Epilepsy Curr. **4**, 65–70 (2004)

54.40 S. Ganesh, R. Puri, S. Singh, S. Mittal, D. Dubey: Recent advances in the molecular basis of Lafora's progressive myoclonus epilepsy, J. Hum. Gener. **51**, 1–8 (2006)

54.41 L.F. Abbott, K.A. Thoroughman, A.A. Prinz, V. Thirumalai, E. Marder: Activity-dependent modifications of intrinsic and synaptic conductances in neurons and rhytmic networks. In: *Modeling Neural Development*, ed. by A. van Oojen (MIT Press, Cambridge 2003) pp. 151–166

54.42 G. LeMasson, E. Marder, L.F. Abbott: Activity-dependent regulations of conductances in model neurons, Science **259**, 1915–1917 (1993)

54.43 L. Benuskova, V. Jain, S.G. Wysoski, N. Kasabov: Computational neurogenetic modeling: A pathway to new discoveries in genetic neuroscience, Int. J. Neural. Syst. **16**, 215–227 (2006)

54.44 L. Benuskova, N. Kasabov: Modeling brain dynamics using computational neurogenetic approach, Cogn. Neurodyn. **2**, 319–334 (2008)

54.45 H. Lodish, A. Berk, S.L. Zipursky, P. Matsudaira, D. Baltimore, J. Darnell: *Molecular Cell Biology*, 5th edn. (Freeman, New York 2000), Chap. 4: Nucleic acids, the genetic code, and the synthesis of macromolecules, pp. 100–137

54.46 H. Lodish, A. Berk, S.L. Zipursky, P. Matsudaira, D. Baltimore, J. Darnell: *Molecular Cell Biology*, 5th edn. (Freeman, New York 2000), Chap. 17: Protein sorting: Organelle biogenesis and protein secretion. pp. 675–750

54.47 A.M. Marini, S.J. Rabin, R.H. Lipsky, I. Mocchetti: Activity-dependent release of brain-derived neurotrophic factor underlies the neuroprotective effect of *N*-methyl-D-aspartate, J. Biol. Chem. **273**, 29394–29399 (1998)

54.48 H. Husi, M.A. Ward, J.S. Choudhary, W.P. Blackstock, S.G.N. Grant: Proteomic analysis of NMDA receptor-adhesion protein signaling complexes, Nat. Neurosci. **3**, 661–669 (2000)

54.49 T.P. Garrington, G.L. Johnson: Organization and regulation of mitogen-activated protein kinase signaling pathways, Curr. Op. Cell Biol. **11**, 211–218 (1999)

54.50 P. Baldi, S. Brunak: *Bioinformatics. A Machine Learning Approach*, 2nd edn. (MIT Press, Cambridge 2001)

54.51 J. Bower, H. Bolouri (Eds.): *Computational Modelling of Genetic and Biochemical Networks* (MIT Press, Cambridge 2001)

54.52 L. Chen, K. Aihara: Stability analysis of genetic regulatory networks with time delay, IEEE Trans. Circuits. Syst. – I: Fundam. Theory Appl. **49**, 602–608 (2002)

54.53 L.F.A. Wessels, E.P. van Someren, M.J.T. Reinders: A comparison of genetic network models, Proc. Pac. Symp. Biocomput., Vol. 6 (World Scientific, Singapore 2001) pp. 508–519

54.54 P. D'Haeseleer, X. Wen, S. Fuhrman, R. Somogyi: Linear modeling of mRNA expression levels during CNS development and injury, Proc. Pac. Symp. Biocomput., Vol. 4 (World Scientific Publ., Singapore 1999) pp. 41–52

54.55 J. Norbury, R.E. Wilson: Dynamics of constrained differential delay equations, J. Comput. Appl. Math. **125**, 201–215 (2000)

54.56 L.D. Drager, W. Layton: Initial value problems for nonlinear nonresonant delay differential equations with possibly infinite delay, Electron J. Differ. Equ. **24**, 1–20 (1997)

54.57 D. Greenbaum, C. Colangelo, K. Williams, M. Gerstein: Comparing protein abundance and mRNA expression levels on a genomic scale, Genome Biol. **4**, 117111–117118 (2003)

54.58 R. Jansen, D. Greenbaum, M. Gerstein: Relating whole-genome expression data with protein-protein interactions, Genome Res. **12**(1), 37–46 (2002)

54.59 M. Thoby-Brisson, J. Simmers: Transition to endogenous bursting after long-term decentralization requires de novo transcription in a critical time window, J. Neurophysiol. **84**, 596–599 (2000)

54.60 G. Turrigiano, G. LeMason, E. Marder: Selective regulation of current densities underlies spontaneous changes in the activity of cultured neurons, J. Neurosci. **15**, 3640–3652 (1995)

54.61 W. Gerstner, W.M. Kistler: *Spiking Neuron Models* (Cambridge Univ. Press, Cambridge 2002)

54.62 W. Maass, C.M. Bishop (Eds.): *Pulsed Neural Networks* (MIT Press, Cambridge 1999)

54.63 I.C. Kleppe, H.P.C. Robinson: Determining the activation time course of synaptic AMPA receptors from openings of colocalized NMDA receptors, Biophys. J. **77**, 1418–1427 (1999)

54.64 S. Charpier, H. Leresche, J.-M. Deniau, S. Mahon, S.W. Hughes, V. Crunelli: On the putative contribution of $GABA_B$ receptors to the electrical events occuring during spontaneous spike and wave discharges, Neuropharmacology **38**, 1699–1706 (1999)

54.65 R.A. Deisz: $GABA_B$ receptor-mediated effects in human and rat neocortical neurones in vitro, Neuropharmacology **38**, 1755–1766 (1999)

54.66 M. Beierlein, C.P. Fall, J. Rinzel, R. Yuste: Thalamocortical bursts trigger recurrent activity in neocortical networks: Layer 4 as a frequency-dependent gate, J. Neurosci. **22**, 9885–9894 (2002)

54.67 N. Kasabov, Z.S.H. Chan, V. Jain, I. Sidorov, D.S. Dimitrov: Gene regulatory network discovery from time-series gene expression data – a computational intelligence approach, LNCS **3316**, 1344–1353 (2004)

54.68 Z. Chan, N. Kasabov, L. Collins: A hybrid genetic algorithm and expectation maximization method for global gene trajectory clustering, J. Bioinform. Comput. Biol. **3**, 1227–1242 (2005)

54.69 D.J. Whitehead, A. Skusa, P.J. Kennedy: Evaluating an evolutionary approach for reconstructing gene regulatory networks, Proc. 9th Int. Conf. Simul. Synth. Living Syst. (ALIFE9) (MIT Press, Boston 2004)

54.70 F.X. Wu, W.J. Zhang, A.J. Kusalik: Modeling gene expression from microarray expression data with state-space equations, Proc. Pac. Symp. Biocomput., Vol. 9 (World Scientific, Singapore 2004) pp. 581–592

54.71 M.B. Elowitz, S. Leibler: A synthetic oscillatory network of transcriptional regulators, Nature **403**, 335–338 (2000)

54.72 E.A. Thomas, C.A. Reid, S.F. Berkovic, S. Petrou: Prediction by modeling that epilepsy may be caused by very small functional changes in ion channels, Arch. Neurol. **66**(10), 1225–1232 (2009)

54.73 V. Santhakumar, I. Aradi, I. Soltesz: Role of mossy fiber sprouting and mossy cell loss in hyperexcitability: A network model of the dentate gyrus incorporating cell types and axonal topography, J. Neurophysiol. **93**(1), 437–453 (2005)

54.74 R.J. Morgan, I. Soltesz: Nonrandom connectivity of the epileptic dentate gyrus predicts a major role for neuronal hubs in seizures, Proc. Natl. Acad. Sci. USA **105**(16), 6179–6184 (2008)

54.75 N. T. Carnevale, M.L. Hines: NEURON simulation environment (2011), available online at http://www.neuron.yale.edu/neuron/ (last accessed 3 May 2013)

54.76 Ingenuity Systems, Inc.: Ingenuity pathway analysis (IPA) (2011), available online at http://www.ingenuity.com/index.html (last accessed 3 May 2013)

54.77 H. Caspers: Mechanisms of EEG generation – historical and present aspects. In: *Basic Mechanisms of the EEG*, ed. by S. Zschocke, E.-J. Speckmann (Birkhauser, Boston 1993)

54.78 H. Lodish, A. Berk, S.L. Zipursky, P. Matsudaira, D. Baltimore, J. Darnell: *Molecular Cell Biology*, 5th edn. (Freeman, New York 2000), Chap. 8: Genetic analysis in cell biology, pp. 254–293

54.79 R. Morita, E. Miyazaki, C.G. Fong, X.-N. Chen, J.R. Korenberg, A.V. Delgado-Escueta, K. Yamakawa: JH8, A gene highly homologous to the mouse jerky gene, maps to the region for childhood absence epilepsy on 8q24, Biochem. Biophys. Res. Commun. **248**, 307–314 (1998)

54.80 L.T. MacNeil, J.M. Walhout: Gene regulatory networks and the role of robustness and stochasticity in the control of gene expression, Genome Res. **21**, 645–657 (2011)
54.81 A. Garg, K. Mohanran, A. Di Cara, G. De Micheli, I. Xenarios: Modeling stochasticity and robustness in gene regulatory networks, Bioinformatics **25**, i101–i109 (2009)
54.82 M. Aldana, E. Balleza, S. Kauffman, O. Resendiz: Robustness and evolvability in genetic regulatory networks, J. Theor. Biol. **245**, 433–448 (2007)
54.83 S. Ciliberti, O.C. Martin, A. Wagner: Robustness can evolve gradually in complex regulatory gene networks with varying topology, PLoS Comput. Biol. **3**(2), 0164–0173 (2007)